

# RSC Advances



This is an *Accepted Manuscript*, which has been through the Royal Society of Chemistry peer review process and has been accepted for publication.

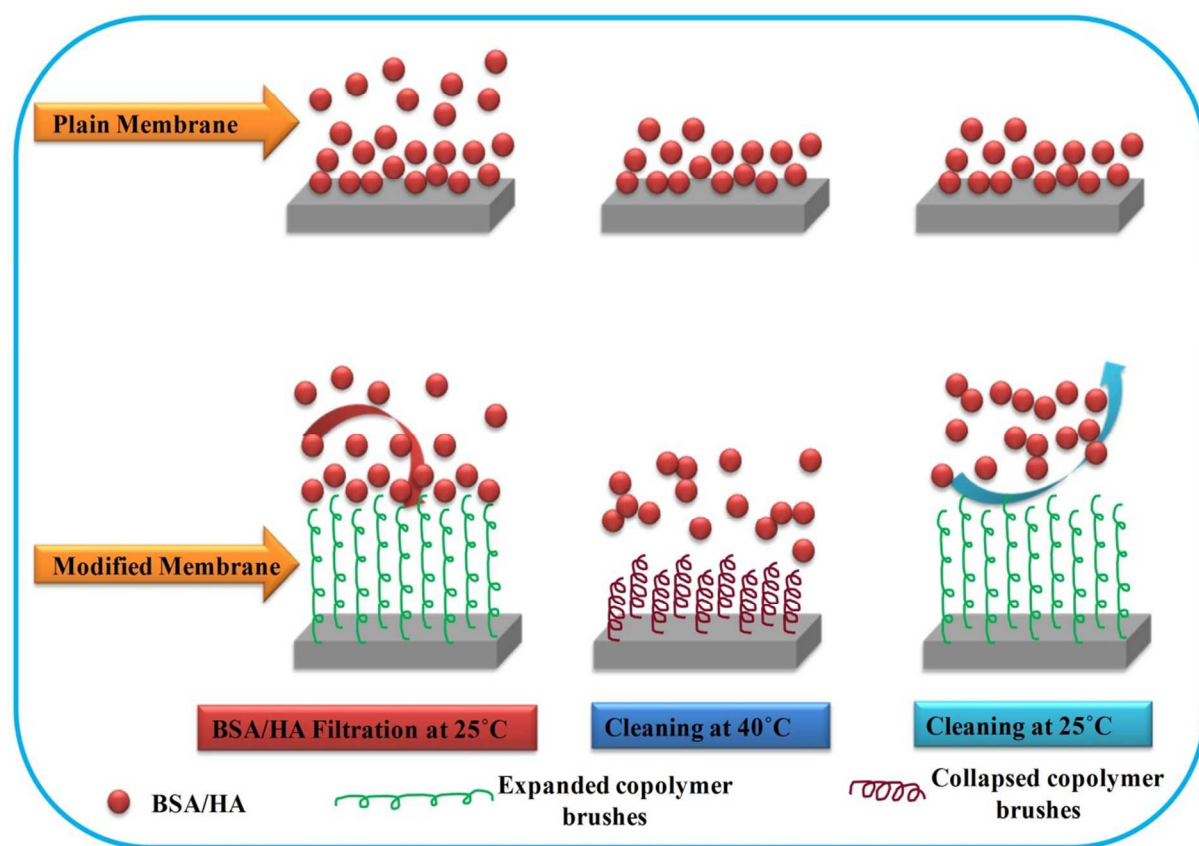
*Accepted Manuscripts* are published online shortly after acceptance, before technical editing, formatting and proof reading. Using this free service, authors can make their results available to the community, in citable form, before we publish the edited article. This *Accepted Manuscript* will be replaced by the edited, formatted and paginated article as soon as this is available.

You can find more information about *Accepted Manuscripts* in the [Information for Authors](#).

Please note that technical editing may introduce minor changes to the text and/or graphics, which may alter content. The journal's standard [Terms & Conditions](#) and the [Ethical guidelines](#) still apply. In no event shall the Royal Society of Chemistry be held responsible for any errors or omissions in this *Accepted Manuscript* or any consequences arising from the use of any information it contains.

**Research Highlights:**

- Amphiphilic thermo responsive PVCL-co-PSF copolymer was synthesized .
- Enhanced pore density and hydrophilicity was achieved.
- Higher hydration capacity and lower BSA adsorption was found.
- 92.5 % and 95 % flux recovery ratio was achieved with BSA and HA, respectively.



Mechanism for stimuli responsive cleaning

**Preparation of novel thermo responsive PSF membrane, with cross linked  
PVCL-co-PSF copolymer for protein separation and easy cleaning**

M. K. Sinha and M. K. Purkait<sup>\*</sup>

Department of Chemical Engineering  
Indian Institute of Technology Guwahati  
Guwahati - 781039, Assam, India

---

<sup>\*</sup> Corresponding author

Tel: + 91 - 361 - 2582262

Fax: +91 - 361 - 2582291

E. Mail: [mihir@iitg.ernet.in](mailto:mihir@iitg.ernet.in)

## Abstract

An amphiphilic thermo responsive cross linked polyvinylcaprolactam-co-polysulfone (PVCL-co-PSF) copolymer was synthesized via solution polymerization of vinylcaprolactam (VCL) in PSF solution by use of three different initial ratio of PSF to VCL monomer. After the synthesis of copolymer, required amount of PSF was dissolved in PVCL-co-PSF copolymer solution. Presence of copolymer in blended membrane was confirmed by Fourier transform infrared-attenuated total reflectance (FTIR-ATR) spectroscopy. Blended membranes showed enhanced pure water flux, hydrophilicity and evident of thermo sensitivity. Hydration capacity for modified membrane decreased from 279 to 161 mg/cm<sup>3</sup> when temperature changed from 25 to 40 °C. The hydration capacity of the modified PSF membrane compared to plain PSF membrane increased from 127 to 279 mg/cm<sup>3</sup>, and the adsorbed protein amount decreased from 0.14 mg/cm<sup>2</sup> to 0.03 mg/cm<sup>2</sup> at 25 °C. Reversible volume phase transition of PVCL around the lower critical solution temperature (LCST) was used as an environmentally-friendly approach for membrane cleaning. Temperature change water elution hydraulic cleaning for modified membranes around the LCST of the PVCL-co-PSF copolymer brushes was proposed (as shown in Figure 7). Following the alternate temperature-change (40 °C/25 °C) cleaning, a flux recovery of about 92.5% (in case of BSA) and 95% (in case of HA) were obtained for the modified PSF membrane (the flux recovery of the plain membrane were only about 39% and 36 % after BSA and HA ultrafiltration, respectively).

**Keywords:** thermo responsive; hydrophilic; fouling resistance; modified cleaning; ultrafiltration.

## 1. Introduction

Ultrafiltration membranes are widely used for environmental and biochemical applications.<sup>1-3</sup> Low energy consumption, lack of phase change, simplicity of operation and compact design are the reason of wide spread use of ultrafiltration membranes. Ultrafiltration membranes are mainly made by polysulfone (PSF)/polyether sulfone (PES) by phase inversion method, due to their good physicochemical stability, resistance to chemical, wide pH range, mechanical and thermal stability.<sup>4</sup> Solubility of PSF makes it ideal membrane material for membrane fabrication by phase inversion method. Apart from this, durability of PSF membranes makes them ideal choice for general filtration purpose.<sup>5</sup> However; major drawback of PSF membranes is their hydrophobic nature. Due to the hydrophobicity, matters in water like natural organic matter, protein and oils deposited onto the membrane surface or inside the pores, this amplify the hydraulic resistance, increases the pressure drop across membrane and reduce the membrane flux.<sup>6</sup>

Significant attempt has been made to overcome this problem and develop mitigation approach to enhance the ultrafiltration membrane performance. Primarily four approaches are used for the modification of PSF ultrafiltration membrane. First two methods are post modification of prepared membrane namely surface grafting via UV induced grafting, redox initiated grafting, plasma treatment and second method is modification of PSF membrane by thin film coating.<sup>7, 8</sup> The main disadvantages of these two methods are the additional complicated steps as well as these methods severely alter the pore size and pore size distribution of membranes whereas internal pores are barely modified. Third method is related to pre functionalization of PSF by addition of hydrophilic functional group to PSF chain like carboxylation, sulphonation and amination.<sup>9-11</sup> Fourth and most preferred method is blending of additive in membrane casting solution.

Usually two types of additives are used, inorganic materials and organic materials. Inorganic material includes various kinds of metal oxide nanoparticles like  $\text{TiO}_2$ ,  $\text{Al}_2\text{O}_3$ ,  $\text{SiO}_2$  and  $\text{ZnO}$ . Addition of nanoparticles in polymeric membrane matrix improves the wettability, hydrophilicity and fouling resistant behaviour. But, with the addition of nanoparticles, reduction in flux was observed. Reason for water flux reduction was agglomeration of nanoparticles, which resulted in pore blockage.<sup>12-14</sup> So, blending of organic material with desired property is an important alternate and it is less complicated and economical process compared to all other techniques. Various organic materials like water soluble polymer, hydrophilic polymers and charged polymers have been mixed together with membrane casting solution. Among various additives, polyvinylpyrrolidone and polyethylene glycol are most favourable for membrane modification by blending due to their protein resistant character.<sup>15, 16</sup> But, due to water soluble nature, these polymers ultimately leach out from the membrane surface after some time of use.<sup>17</sup> To overcome this deficiency amphiphilic copolymers were introduced in membrane casting solution. While hydrophobic segment of amphiphilic additive has the affinity for the host hydrophobic polymer (like PSF) and it ensured the copolymers to be securely anchored in the host polymer matrix. On the other side, hydrophilic segment in copolymer endowed the membrane surface with improved hydrophilicity.<sup>18</sup>

But the problem is, once the foulants get deposited on membrane surface, the modified surface no longer remains efficient in checking the fouling. The membrane surface and solute particle interaction did not remain the same with the formation of fouling layer and due to the changed property, it cannot prevent the further deposition of foulants.<sup>19</sup> In conventional fouling resistance membranes, the fouling resistant additives or layer on the membrane surface remain stagnant and foulants get deposited on these additives, after some time of use. It is difficult to remove the foulants from those deposited areas due to the

sluggish property of these additives. So, to remove these foulants from deposited areas chemical cleaning is applied. Chemical cleaning of membranes reduces the effectiveness and selectivity as well as life time of membranes. Thus, to overcome these issues stimuli responsive materials are used to blend with casting solution of membranes. These stimuli responsive materials are responsive to change in temperature, pH, ion concentration etc. The swelling and shrinking properties of the stimuli responsive materials, helps in membrane cleaning by simple hydraulic cleaning. As, due to shrink and swell behaviour, the deposited foulants layer get damaged and can be removed by hydraulic cleaning. Previously we have prepared a pH responsive membrane by adding pegylated functional copolymer poly (acrylic acid-co-polyethylene glycol methyl ether methacrylate).<sup>20</sup> This additive had provided excellent anti fouling resistance behaviour.

In the present study cross-linked polyvinylcaprolactam-co-polysulfone (PVCL-co-PSF) amphiphilic copolymer was synthesized by taking different initial ratio of PSF to vinylcaprolactam (VCL) monomer. Azobisisobutyronitrile (AIBN), N,N'-methylenebisacrylamide (MBAA) and N-methylpyrrolidone (NMP) were used as initiator, cross-linker and solvent, respectively. In this copolymer, PVCL is a well known thermo responsive polymer, with lower critical solution temperature (LCST) around ( $\approx 34^\circ\text{C}$ ).<sup>21</sup> It is usually used for the control drug release applications.<sup>22, 23</sup> Above the LCST, it remains in swollen state and below this temperature it rejects absorbed water and comes to shrunken state. In current study, the thermo responsive behaviour of PVCL was capitalized for hydraulic cleaning and rinsing by keeping the membrane at two temperatures i.e. at  $25^\circ\text{C}$  and  $40^\circ\text{C}$ , alternately. PSF segment of the copolymer has the natural affinity for base membrane polymer due to hydrophobic nature and kept the copolymers to be securely attached to membrane surface. Also, due to amphiphilic behaviour of the copolymer it is expected that in the membrane casting solution the hydrophilic (PVCL) segment of copolymer located at the

upper interface will be oriented toward the liquid. This provides a more hydrophilic environment. Hydrophobic segment should be in the contact with air. After the immersion of casting solution in coagulation bath, phase inversion has been prompted and copolymer molecules are rearranged up-side down. Certainly, the polymer system becomes more hydrophobic due to the outflow of solvent. At the end, hydrophobic segment interact with PSF while hydrophilic segments should be oriented toward the top surface. Apart from that, copolymer molecules initially present in the bulk solution phase may migrate toward the top surface of membrane during phase inversion.<sup>24</sup> The coupling of environmentally responsive polymers in PSF membranes allows to rapid change in presence of stimuli as it synergizes the chemical stability and mechanical strength of the polymer chain. Hence, responsive membranes enable changing their effective pore size and mechanical properties such as Young's modulus under varying stimuli responsive environment like temperature and pH.

Composition and morphology of the fabricated membranes were analyzed by ATR-FTIR, SEM and FESEM. Hydration capacity, water flux, hydraulic permeability, UF performance and anti fouling property of modified membranes were investigated using bovine serum albumin (BSA) and humic acid (HA). Proxy organic materials have commonly been used to represent wastewater effluent organic matter (EfOM), natural organic matter (NOM) and soluble microbial products (SMP) in study of membrane fouling. Here, HA was used as EfOM and NOM foulant, whereas BSA was used as SMP.<sup>25, 26</sup>

## 2. Experimental

### 2.1. Materials

PSF (average  $M_w = 35000 \text{ gmol}^{-1}$ ), N,N'-methylenebisacrylamide (MBAA), humic acid (HA) and monomer N-vinylcaprolactam (VCL) were purchased from Sigma-Aldrich Co. USA. Reagent grade N-methylpyrrolidone (NMP) was supplied by LOBA Chemie, India.



PEG4000 were purchased from Merck-India. Bovine serum albumin (BSA) with molecular weight of 68,000 Da and azobisisobutyronitrile (AIBN) were obtained from Otto Chemie Private Limited, India. Deionized (DI) water purified by Millipore system (Millipore, France) was used throughout the experiments.

## **2.2. Synthesis of PVCL-co-PSF copolymer and fabrication of modified PSF membranes**

The cross-linking of VCL in PSF solution was carried out by free radical polymerization of VCL in NMP solvent. Azoisobutyronitrile (AIBN) was used as the initiator and N, N'-methylene bisacrylamide (MBAA) was used as the cross-linking reagent. All the reactants i.e. VCL, PSF, MBAA, AIBN and NMP were taken in a three neck round bottom flask. The reaction mixture was purged with pure nitrogen gas to remove oxygen which could act as a scavenger in the radical polymerization. After purging with nitrogen gas, polymerization reaction was carried at 70 ° C for 24 h. After the completion of reaction required amount of PSF and PEG4000 was directly dissolved in PVCL-co-PSF copolymer solution, so that the total concentration of PSF was 15 % and that of PEG4000 was 7 %. This mixture was vigorously mixed at 50 ° C for 12 h and further degassed for 6 h at 50 ° C. The solution was then cast on a clean glass plate with a casting knife maintaining a uniform thickness of 200 µm, in the ambient atmosphere. Afterwards the casted membrane was immersed into the coagulation bath at room temperature. The prepared membranes were kept in fresh DI water for overnight to eliminate any residual solvent. Finally, membrane sheets were air dried at room temperature. Steps for the fabrication of modified membranes are shown in figure 1.

## **2.3. Membrane characterization**

The presence of cross linked PVCL-co-PSF copolymer in blended membrane was confirmed by ATR-FTIR (IRAffinity-1, Shimadzu, Japan). FTIR analysis was done with 30 numbers of scans with apparatus resolution of 4. Morphological study of the plain and modified membranes was done by FESEM (Make: Zeiss LSM 510 Meta). Water contact angle (CA) between membrane surface and water droplet is the measure of the hydrophilicity of the membrane surface, smaller the contact angle, higher the hydrophilicity of the surface. Average of 8 contact angle measurements was considered for all the prepared membranes. Hydration capacity of the fabricated membranes was also studied in terms of amount of absorbed water per unit volume of membranes ( $\text{mg}/\text{cm}^3$ ). Weight of  $4 \text{ cm}^2$  membrane was first measured in dry state. Thereafter, membrane was immersed in water for 12 h. Subsequently, after mopping the surface water with tissue paper, membranes were weighted in wet state. Hydration capacity was calculated by taking the difference of dry and wet weights per unit volume. Four different tests were performed and the average was taken for each membrane. Thickness of the membranes for calculation of volume of membranes were measured by a digimatic measuring unit (model: Litematic, VL 50, Mitutoyo, Japan) at 10 different places and average was taken. The adsorption of BSA on membrane surface is an important parameter for the estimation of fouling behaviour of membranes. First of all, membranes were placed in 5 ml vials and were soaked in 4 ml of phosphate buffer for 1 h at  $25^\circ \text{C}$ . After that, buffer was removed and membranes were incubated with 4 ml of 1000 PPM BSA solution for 12 h at  $25^\circ \text{C}$ . The absorbed amount of BSA was measured by UV-VIS spectrophotometer at wavelength of 280 nm. Three duplicate tests were performed for each membrane.

#### **2.4. Pure water permeation and filtration experiments**

All the membranes were compacted for 2 h at transmembrane pressure of 300 kPa and flux was measured at regular interval. After the compaction water permeation through all the membranes at different pressure was measured and hydraulic permeability ( $L_m$ ) was measured using that data. The pure water flux (PWF) was measured by using the following equation:

$$J_w = \frac{V}{A\Delta t} \quad (1)$$

Here,  $J_w$  is pure water flux ( $L/m^2$  h),  $V$  is the volume of water permeated (L),  $A$  is the effective membrane area ( $m^2$ ) and  $\Delta t$  is permeation time (h). Hydraulic permeability ( $L_m$ ) ( $L/m^2$  h kPa) is calculated from the slope of the plot of  $J_w$  vs  $\Delta P$  from the following equation:

$$L_m = \frac{J_w}{\Delta P} \quad (2)$$

For evaluation of fouling due to BSA and HA ultrafiltration, all the membranes were first compacted at 300 kPa for 30 minute. Then pressure was reduced to 250 kPa and pure water flux was measured at regular interval for 90 minutes. Flux at the end of 90 minute was termed as  $J_{w1}$ . Subsequently feed was changed with 1000 mg/L BSA/HA solution and BSA/HA flux was measured for next 90 minutes. BSA/HA flux at the end of this 90 minute was called as  $J_p$ . BSA and HA rejections were measured with UV-VIS spectroscopy at 280 nm and 254 nm, respectively by using following formulae:

$$R(\%) = \left( 1 - \frac{C^{permeate}}{C^{feed}} \right) \times 100 \quad (3)$$

Here,  $C^{permeate}$  and  $C^{feed}$  represents BSA/HA concentration in permeate and feed respectively. After BSA/HA ultrafiltration, membrane was washed with pure water flushing, and then again pure water was permeated through membrane for 90 minutes. The water flux at the end of this 90 minute was labelled as  $J_{w2}$ .

### 3. Results and discussion

#### 3.1. FTIR analysis

Figure 2 shows ATR-FTIR spectra of plain and blended PSF membranes surfaces fabricated with different initial ratio of PSF and VCL monomer. The peaks at  $1158\text{ cm}^{-1}$  and  $1287\text{ cm}^{-1}$  are due to  $-\text{C}-\text{O}-\text{C}-$  and  $\text{S}=\text{O}$  group present in PSF, thus verifying the presence of PSF. A new peak become visible around  $1529\text{ cm}^{-1}$ , confirms the presence of secondary amide group present in  $\text{N},\text{N}'$ -methylenebisacrylamide (used as cross linker for PVCL-co-PSF copolymer). The most important change is the emergence of new peaks at around  $1658\text{ cm}^{-1}$   $1476\text{ cm}^{-1}$  which confirms the presence of PVCL in membrane matrix. The peak at  $1476\text{ cm}^{-1}$  is due to  $-\text{CH}-$  group attached to nitrogen atom on PVCL structure and the peak at  $1658\text{ cm}^{-1}$  is due to the tertiary amide group present in PVCL segment of copolymer. The intensity of these peaks is much higher for membrane  $\text{M}_{15}$  compared to  $\text{M}_{05}$ , it means membrane  $\text{M}_{15}$  has more amount of PVCL segment present in copolymer, as VCL monomer was present in higher ratio for initial cross linking polymerization reaction for membrane  $\text{M}_{15}$  compared to membrane  $\text{M}_{05}$ .

#### 3.2. Membrane hydration, hydrophilicity and BSA adsorption studies

Figure 3 shows the effect of initial ratio of PSF and VCL monomer on hydration capacity of membranes. The measured quantity of the hydration capacity is result of trapping of water in porous structure of membrane, binding of water molecules around the hydrophilic segment of amphiphilic brushes and entrapped water molecules in the confined spaces between amphiphilic chains. So, hydration capacity of the plain membrane was attributed to only porous structure compared to the blended membranes. In addition, Table 2 is reporting the growth of membrane thickness as function of PVCL content. It supported that PVCL-PSF copolymer prevent the shrinkage of the membrane during membrane formation. Thus, the

increases in initial ratio of VCL monomer associated with the increase in amount of hydrophilic brush like structure due to the self rearrangement of amphiphilic PVCL-co-PSF copolymer on the membrane surface. This in result increased the hydration capacity, which is dependent on the bound and entrapped water molecules. So, the formation of bound water layer on blended membrane was regarded as vital to repel proteins and generate the bio fouling resistant surface.

Figure 3 also shows the hydration capacity of the prepared membranes at 25 °C and 40 °C. It is well known that PVCL has lower critical solution temperature (LCST) of ~ 35 °C, which gives thermo responsive property to the copolymer and hence provides thermo responsive behaviour to the modified membrane. This thermo responsive property of the PVCL is present due to the configurational changes in PVCL chain. Below the LCST, the PVCL polymer chains adopted an extended random coils configuration (increased membrane porosity) and absorb more amount of water within its coil type configuration. Whereas at temperature above LCST, the PVCL polymer chains shrank to form a compact structure (less membrane porosity) and dehydrated the absorbed water.<sup>27, 28</sup> Due to this swell and shrink function of PVCL, hydration capacity of modified membrane changes below and above LCST.

Bio-foulants like BSA strongly interacts with hydrophobic membrane surfaces and thereby causes significant water flux decline by fouling during the ultrafiltration. In this regard, it is of major concern to fabricate membranes with ability to resist protein adsorption. The physical deposition of foulants can be reduced by increasing the membrane surface hydrophilicity. Water contact angle (WCA) and adsorb BSA quantity for different membranes are shown in Figure 4. Hydrophilic behaviour of the membrane is explained by water contact angle measurement. Lower the WCA value higher will be the hydrophilicity of the membranes and more hydrophilic membranes are less prone towards fouling. Therefore,

WCA is a significant parameter in membrane separation process and very much related to membrane's fouling behaviour. For unmodified membrane WCA is  $67.5^\circ$  and for membrane  $M_{15}$  it decreased considerably to  $49.5^\circ$ . It is well known that in the presence of hydrophilic functional group like amide group enhances the hydrophilic behaviour of membranes. So, as the quantity of PVCL increases, hydrophilicity of the modified membranes also increases.

It has been discussed that with the increase in initial ratio of VCL monomer, surface hydrophilicity had increased for blended membranes. Though, the estimation of protein adsorption on the membrane surfaces should be considered not only with respect to surface hydrophilicity but also with respect to the hydration capacity of the membranes.<sup>29</sup> It is reported that, the formation of the bound water layer on a surface is considered crucial to repel protein and generate anti-bio fouling surface.<sup>30,31</sup> Figure 4 shows the adsorption of BSA as a function of PVCL content in membranes. The addition of amphiphilic PVCL-co-PSF macromolecule reduces the adsorption of BSA from  $0.145 \text{ mg/cm}^2$  for plain membrane to  $0.025 \text{ mg/cm}^2$  for  $M_{15}$  membrane. These values are lower than some of the reported work by Venault et al.<sup>32</sup> They have reported that the adsorption of BSA for modified membrane was reduced from  $0.18$  to  $0.045 \text{ mg/cm}^2$  compared to plain membrane. 60 % reduction in BSA adsorption was also found by Venault et al.<sup>33</sup> in their separate studies. These values were lower than that of the present work where 82% reduction in BSA adsorption was obtained. On the other hand hydration capacity of membrane increases dramatically with the addition of PVCL-PSF, for plain membrane hydration capacity value is around  $125 \text{ mg/cm}^3$ , whereas for the membrane  $M_{15}$  that value is around  $280 \text{ mg/cm}^3$  at  $25^\circ \text{C}$ . These indicated that with increase in initial quantity of VCL monomer, the membrane became more hydrophilic and hydration capacity was reduced which dictated the lower BSA adsorption amount. The results also confirmed that blending the amphiphilic PVCL-co-PSF copolymer could stem the

adsorption of protein molecules, since hydrophilic copolymer could restrain the protein adsorption amount by forming bound hydration layer on membrane surface.

### 3.3. Microscopic studies

Figure 5 and 6 show the top surface FESEM images and cross sectional images of the plain and blended PSF membranes with different initial ratio of PSF to VCL monomer. The pore size was estimated from the FESEM images by using well known “Image J” software<sup>34</sup> and average pore size for all the membranes was around 25 – 30 nm. One can observe that the membrane M<sub>15</sub> has higher pore density compared to plain membrane and also compared to other modified membranes. It has been stated that amphiphilic or hydrophilic additives would help in pore formation and also segregate at the membrane surface.<sup>35, 36</sup> And, in case of the membrane M<sub>15</sub> the ratio of hydrophilic part in amphiphilic copolymer is higher, so it further induces the pore formation in the membrane M<sub>15</sub>. In case of cross sectional morphology, all the membranes exhibit asymmetric structure. All the fabricated membranes have top dense layer or skin layer supported by porous sub-layer consists of finger like structure and bottom layer. These structures formed due to the high mutual affinity of NMP for water, which results instantaneous demixing.<sup>34</sup>

However, significant change in the finger like structure of the modified membrane can be observed. In case of plain membrane, there are different layers of finger like structure and over all thickness of porous sub layer is more compared to bottom layer. Whereas, in case of membrane M<sub>05</sub> (less quantity of PVCL), finger like structure coalesced together and form bigger finger like structure, but thickness of the porous sub layer in membrane M<sub>05</sub> is still less than plain membrane. Further, in case of the membranes M<sub>10</sub> and M<sub>15</sub>, those fingers like structure became shorter and converted to porous sponge like structure (membrane M<sub>15</sub>).

It is reported that membrane structure is formed by driving force between nonsolvent and solvent and their relative diffusion rate.<sup>37, 38</sup> If there is strong affinity between solvent and nonsolvent then in such condition out diffusion rate of solvent is much higher than the in diffusion rate of nonsolvent. Thus dense skin layer is formed and reduces the diffusion rate of nonsolvent into the sub layer, this result in bigger porous sub layer with finger like structure. Whereas, if there is weak affinity between solvent and nonsolvent, the skin layer will be porous and sponge like structure can be formed. Since, PVCL-co-PSF copolymer has amphiphilic property, the addition of the same influences the relative diffusion rate of solvent and non solvent by reducing the affinity between solvent and nonsolvent. Thus, the in diffusion rate of the nonsolvent decreases during phase inversion process at higher PVCL content. This results in porous sponge like sub layer structure just below the dense skin layer.

### 3.4. Pure water permeation and hydraulic permeability studies

Figure 7 shows the effect of initial ratio of PSF and VCL monomer on the compaction profile during time dependent constant pressure (300 kPa) PWF and calculated compaction factor (CF) is shown in Table 2. CF recounts to the structure of membrane sub layer. Higher the CF, more likely the membrane compacts due to presence of large macro voids in the sub layer. It was already seen that modified membranes have smaller voids in sub layer, which reduces the CF of modified membranes compared to plain membranes. PWF declined sharply for all the membranes for up to 45 minutes and after that PWF remains almost constant. Due to compaction the walls of the pores become closer, denser and uniform resulting reduction in pore size as well as the flux during compaction.<sup>39</sup> From the inset of the figure 7 it is found that the steady state PWF increases with increase in ratio of VCL monomer. Steady state flux for plain membrane and membrane M<sub>15</sub> are 103.5L/m<sup>2</sup>h and 127.2 L/m<sup>2</sup>h, respectively. The increase in steady state flux is due to the higher pore density, as shown in Figures 5.



However, increase in flux is not that much; the possible reason is thermo responsive behaviour of modified membranes. Due to the fact that, PVCL segment of copolymer has LCST around 35 °C. So, below this temperature, PVCL remains in swell state, which reduces the effective pore diameter of modified membranes.

Effect of initial ratio of PSF and VCL monomer on PWF of the membrane at different transmembrane pressure is shown in Figure 8. This experiment was done at different transmembrane pressure between 0 - 300 kPa at a difference of 50 kPa. For all the cases, PWF increases almost linearly with increase in pressure. Pressure dependent flux profiles were used to calculate the hydraulic permeability ( $P_m$ ) of the membranes.  $P_m$  was increased from 0.44 to 0.50 L/m<sup>2</sup> h kPa (Table 2) for plain membrane to modified membrane M<sub>15</sub>. Despite the increase in pore density the hydraulic permeability increased marginally due to thermo responsive property of membrane as discussed earlier. These results are in agreement with the findings of compaction studies and temperature dependent hydration capacity of modified membranes.

### 3.5. Ultrafiltration performance and fouling studies

The ultrafiltration performance, antifouling behaviours and easy cleaning properties of PVCL-co-PSF modified membranes were examined by filtering 1000 PPM BSA and 1000 PPM HA solution at constant transmembrane pressure of 250 kPa. Figure 9a and Figure 9b shows the BSA and HA flux–rejection through plain and modified membranes, respectively. PVCL-PSF modified membranes have comparatively much higher flux than plain membranes, indeed membrane M<sub>15</sub> has almost 3 times higher flux than plain membrane in both the cases. Despite the increase in flux, the rejections through modified membranes are on the higher side than plain membrane M<sub>00</sub>. As we have already discussed that amphiphilic PVCL-co-PSF copolymer not only enhances the hydrophilicity but also pore forming

capacity. Also, due to the thermo responsive property of the modified membranes the pore size of the modified membranes were smaller due to expansion of copolymer molecules at the working temperature ( $\approx 25^\circ\text{C}$ ), which was lower than LCST of PVCL as discussed earlier. The PVCL-co-PSF copolymer also helps to form pure water layer on top surface of membranes, which in returns reduces the deposition of BSA molecules on the membrane surface and enhances the flux through modified membranes. In case of UF experiment with HA, flux is almost 1.7 times higher than BSA flux for membrane  $M_{15}$  and rejection for all the membranes is in the range of 90–95 %. The reason is the molecular structure of BSA and HA. The HA molecules could cross-link with each other to form a porous and mesh gel layer. This cross-linked molecular structure can be easily rejected by the membrane, further this porous and mesh like gel layer would result in a lower flux decline compared to BSA.<sup>40, 41</sup> Whereas, the ellipsoidal-shaped BSA could not cross-link and would pass more easily through the membrane surface. Further, the gel layer of BSA is more compact, which could cause more pore blocking in the initial stage of fouling and result in lower flux.<sup>40, 42</sup>

The dynamic fouling resistance experiment was done to study the antifouling property of prepared membranes, and process was recorded at constant transmembrane pressure of 250 kPa and shown in Figure 10. In first step DI water flux was measured and called as  $J_{w1}$ , after that in 2<sup>nd</sup> step 1000 PPM BSA/HA solution was used to permeate through membranes and measured flux was named as  $J_p$ . Again in 3<sup>rd</sup> step after simple hydraulic cleaning, DI water flux was measured and recorded as  $J_{w2}$ . In another case, 3<sup>rd</sup> step was changed with modified hydraulic cleaning (as shown in Figure 11a and 11b), first membrane was hydraulically washed at  $40^\circ\text{C}$  and after that again hydraulically washed at  $25^\circ\text{C}$ . Finally, DI water flux was measured and named as  $J_{w2}'$ . Data of Figure 10 was used for the calculation of total fouling ( $F_t$ ), reversible fouling ( $F_r$ ), irreversible fouling ( $F_{ir}$ ) and flux recovery ratio ( $Flux_{RR}$ ) by using following equation:

$$F_t = 1 - (J_{BSA}/J_{w1}) \quad (4)$$

$$F_r = (J_{w2} - J_{BSA})/J_{w1} \quad (5)$$

$$F_{ir} = (J_{w1} - J_{w2})/J_{w1} \quad (6)$$

$$Flux_{RR}(\%) = \frac{J_{w2}}{J_{w1}} \times 100 \quad (7)$$

As it is already discussed that modified membranes have higher BSA/HA flux than plain membranes, also flux during ultrafiltration of HA is much higher than ultrafiltration of BSA. Apart from that it can be observed that flux in first step is almost similar for all the membranes. But, as the experiment was progressed the difference between the fluxes values through different membranes were tend to increasing. Flux value  $J_{w2}$  for membrane M<sub>15</sub> is much higher than membrane M<sub>00</sub>. Effect of these changing values can be seen in Figure 12a and 12b; it shows the value of different fouling parameters for the prepared membranes. The plain membrane has the highest value of total fouling and irreversible fouling and also lowest value of reversible fouling. Addition of PVCL-co-PSF copolymer resisted the adsorption of BSA molecule inside the membrane pores by increasing the hydrophilicity. Due to this reason, as the initial ratio of VCL monomer to PSF was increased in the modified membrane, the irreversible fouling was started to reduce in modified membranes. Further when modified hydraulic cleaning was applied for membrane cleaning after fouling with BSA/HA, the value of  $F_{ir}$  was further decreased for modified membranes, but for plain membrane  $F_{ir}$  value was same. In modified hydraulic cleaning BSA fouled membrane was first washed with water at 40 °C. Due to LCST of PVCL around 35 ° C, the molecules of PVCL-co-PSF copolymer shrank to form a compact structure and water molecules expelled from the PVCL-co-PSF structure and subsequently deposited BSA/HA layer was damaged. Changing the cleaning

temperature again to 25 °C, tended the expansion of PVCL-co-PSF copolymer chain and stretching the chain come out of the membrane surface. This resulted in the further damaging or loosening of BSA/HA layer, thus increasing the efficiency hydraulic cleaning. So, incorporation PVCL-co-PSF copolymer in membrane matrix reduces the use of traditional chemical cleaning for polymeric membrane, which reduces the efficiency and life time of the membranes. In case of ultrafiltration with HA,  $J_{w2}$  values are lower compared to BSA ultrafiltration, which in result increases the  $F_{ir}$  value after normal hydraulic cleaning. The possible reason is that; as it was discussed earlier fouling by HA causes formation of porous–mesh like gel layer on the membrane surface. So, this porous–mesh like gel layer formed by HA cannot be removed by normal hydraulic cleaning due to cross linking of HA molecules. But, when the modified hydraulic cleaning was applied that deposited mesh like gel layer of HA was get damaged due to shrink and swell behaviour of copolymer. Hence, when the membrane was washed in second stage, the whole layer was removed by water and it can be seen in Figure 10b that  $J_{w2}$  value in the case of HA is higher than BSA. Therefore, irreversible fouling value after modified hydraulic cleaning is less in HA ultrafiltration compared to BSA ultrafiltration, despite the fact that irreversible value after normal hydraulic cleaning in the case of HA ultrafiltration is higher compared to BSA ultrafiltration.

Figure 13 shows the flux recovery ratio of prepared membrane after normal hydraulic cleaning and also after modified hydraulic cleaning. Reduction in irreversible fouling causes increase in flux recovery ratio for the modified membranes. As flux recovery ratio is directly related to irreversible fouling. The flux recovery ratio for the plain membrane is only around 39 %, while it is 84 % for membrane M<sub>15</sub> in case of BSA ultrafiltration and same values are 25 % and 69 % with HA ultrafiltration. The good antifouling performance of the PVCL-PSF blended membrane possibly credited to the presence of large number of amide groups in the surface of modified membranes resulted from rearrangement of the amphiphilic copolymer

towards the top surface of the modified membranes. This results in reduction in water contact angle, increase in hydration capacity and reduction in BSA adsorption (Figure 3 and 4). The more hydrophilic surface cause formation of a water layer and repel the hydrophobic foulants. In case of cleaning by modified method, it further enhances the flux recovery ratio of modified membranes by reducing the value of  $F_{ir}$ , as discussed earlier. The flux recovery ratio of membrane  $M_{15}$  are 92.5 % and 95 % compared to 39 % and 26 % of plain membrane for BSA and HA ultrafiltration, respectively, after cleaning with modified method.

#### 4. Conclusion

Cross linked PVCL-co-PSF amphiphilic copolymer were synthesized by polymerization of VCL with PSF by solution polymerization in NMP using different ratio of PSF: PVCL. PSF was directly blended to this polymerized solution. The blended membranes were characterized by ATR-FTIR, FESEM images, BSA adsorption, water contact angle, PWF and BSA/HA ultrafiltration for fouling studies. Also modified hydraulic cleaning technique was used by varying the temperature of water between 25 and 40 °C. The results are summarized as follows: (a) Membranes modified with PVCL-PSF copolymer showed the visible thermo sensitivity as hydration capacity of membrane  $M_{15}$  increased from 160 mg/cm<sup>3</sup> to 280 mg/cm<sup>3</sup>, when temperature was changed from 40 °C to 25 °C. (b) Top surface FESEM images of modified membranes showed the uniform pore size distribution and as well increase in pore density for modified membrane. (c) Cross sectional FESEM images showed that all the membranes had asymmetric structure with visible change in finger like structure. (d) Blending of PVCL-co-PSF amphiphilic copolymer increases the hydrophilicity and reduces the BSA adsorption on membrane surface. (e) Modified hydraulic cleaning increased the flux recovery ratio considerably compared to normal hydraulic cleaning. Flux recovery ratio of membrane  $M_{15}$  improved from 84 % to 92.5 % in case of BSA ultrafiltration and

from 69 % to 95 % in case of HA ultrafiltration, when cleaning process of membranes were changed from normal hydraulic to modified hydraulic cleaning. (f) Modified hydraulic cleaning was more effective in case of membrane fouled during HA ultrafiltration.

### **Acknowledgement**

This work is partially supported by a grant from the Indian National Science Academy (INSA), New Delhi. Any opinions, findings and conclusions expressed in this paper are those of the authors and do not necessarily reflect the views of INSA, New Delhi.

**References**

- 1 S. S. Madaeni, *Water Research*, 1999, **33**, 301-308.
- 2 R. Ghosh and Z.F. Cui, *J. Membr. Sci.*, 2000, **167**, 47–53.
- 3 D. Wu and M. R. Bird, *J. Food Proc. Eng.*, 2007, **30**, 293–323.
- 4 Y. Zhang, Z. Jin, X. Shan, J. Sunarso and P. Cui, *J. Hazard. Mater.*, 2011, **186**, 390–395.
- 5 J.C. Schrotter and B. B. Schrotter, *Current and Emerging Membrane Processes for Water Treatment*, Wiley-VCH, New York, 2010.
- 6 I. N. H. M. Amin, A. W. Mohammad, M. Markom, C.P. Leo and N. Hilal, *J. Membr. Sci.*, 2010, **351**, 75–86.
- 7 S. Belfer, J. Gilron, Y. Purinson, R. Fainshtain, N. Daltrophe, M. Priel, B. Tenzer and A. Toma, *Desalination*, 2001, **139**, 169–176.
- 8 N. Nady, M.C.R. Franssen, H. Zuilhof, M.S.M. Eldin, R. Boom, and K. Schroën, *Desalination*, 2011, **275**, 1-9.
- 9 Y. H. Cho, J. Han, S. Han, M. D. Guiver and H. B. Park, *J. Membr. Sci.*, 2013, **445**, 220–227.
- 10 D. L. Arockiasamy, A. Nagendran, K. H. Shobana and D. Mohan, *Sep. Sci. Technol.*, 2009, **44**, 398–421.
- 11 R. Malaisamy, R. Mahendran, D. Mohan, M. Rajendran and V. Mohan, *J. Appl. Polym. Sci.*, 2002, **86**, 1749–1761.
- 12 A. Razmjou, J. Mansouri and V. Chen, *J. Membr. Sci.*, 2011, **378**, 73–84.
- 13 C. P. Leo, W. P. C. Lee, A. L. Ahmad and A. W. Mohammad, *Sep. Purif. Technol.*, 2012, **89**, 51–56.
- 14 N. Maximous, G. Nakhla, W. Wan and K. Wong, *J. Membr. Sci.*, 2009, **341**, 67–75.
- 15 A. Idris, N. M. Zain and M. Y. Noordin, *Desalination*, 2007, **207**, 324–339.

- 16 B. Chakrabarty, A. K. Ghoshal, and M. K. Purkait, *J. Membr. Sci.*, 2008, **315**, 36–47.
- 17 N. Pezeshk, D. Rana, R.M. Narbaitz and T. Matsuura, *J. Memb. Sci.*, 2012, **389**, 280–286.
- 18 W. Zhao, Y.L. Su, Ch. Li, Q. Shi, X. Ning and Z.Y. Jiang, *J. Membr. Sci.*, 2008, **318**, 405–412.
- 19 D. Rana and T. Matsuura, *Chem. Rev.*, 2010, **110**, 2448–2471
- 20 M. K. Sinha and M. K. Purkait, *J. Memb. Sci.*, 2014, **464**, 20–32.
- 21 X. Jiang, G. Lu, C. Feng, Y. Li and X. Huang, *Polym. Chem.*, 2012, **4**, 3876–3884.
- 22 K. M. Rao, B. Mallikarjuna, K. S. V. K. Rao, S. Siraj, K. C. Rao and M.C.S. Subha, *Colloids Surf. B. Biointerfaces.*, 2013, **102**, 891–897.
- 23 T. Kavitha, I. K. Kang and S. Y. Park, *Colloids Surf. B. Biointerfaces.*, 2014, **115**, 37–45.
- 24 C. H. Loh, R. Wang, L. Shi and A. G. Fane, *J. Membr. Sci.*, 2011, **380**, 114–123.
- 25 Q. Yang, Y. Liu and Y. Li, *J. Membr. Sci.*, 2010, **364**, 372–379.
- 26 H. C. Kim and B. A. Dempsey, *J. Membr. Sci.*, 2013, **428**, 190–197.
- 27 A. Pich, A. Tessier, V. Boyko, Y. Lu and H. P. Adler, *Macromolecules*, 2006, **39**, 7701–7707.
- 28 X. Jiang, G. Lu, C. Feng, Y. Li and X. Huang, *Polym. Chem.*, 2012, **4**, 3876–3884.
- 29 Y. Chang, Y. J. Shih, C. Y. Ko, J. F. Jhong, Y. L. Liu and T. C. Wei, *Langmuir*, 2011, **27**, 5445–5455.
- 30 Y. Chang, W. L. Chu, W. Y. Chen, J. Zheng, L. Liu, R.C. Ruaan and A. Higuchi, *J. Biomed. Mater. Res.*, 2010, **93A**, 400–408.
- 31 S. Krishnan, C. J. Weinman and C. K. Ober, *J. Mater. Chem.*, 2008, **18**, 3405–3413.
- 32 A. Venault, Y. Chang, H. S. Yang, P. Y. Lin, Y. J. Shih and A. Higuchi, *J. Membr. Sci.*, 2014, **454**, 253–263.



- 33 A. Venault, Y. Chang, D. M. Wang and J. Y. Lai, *J. Memb. Sci.*, 2012, **423-424**, 53–64.
- 34 M. K. Sinha and M. K. Purkait, *J. Memb. Sci.*, 2013, **437**, 7–16.
- 35 J. F. Hester, P. Banerjee, Y. Y. Won, A. Akthakul, M. H. Acar and A. M. Mayes, *Macromolecules*, 2002, **35**, 7652–7661.
- 36 X. L. Ma, Y. L. Su, Q. Sun, Y. Q. Wang and Z. Y. Jiang, *J. Membr. Sci.*, 2007, **292**, 116–124.
- 37 R.M. Boom, I.M. Wienk, T. Boomgaard and C.A. Smolders, *J. Membr. Sci.*, 1992, **73**, 277-292.
- 38 J. H. Kim and K. H. Lee, *J. Membr. Sci.*, 1998, **138**, 153-163.
- 39 M. Mulder, *Basic Principles of Membrane Technology*, Kluwer Academic Publishers, Dordrecht, 1991.
- 40 R. Miao, L. Wang, L. Feng, Z. W. Liu and Y. T. Lv, *Desalin. Water Treat.*, 2013, **52**, 5061–6067.
- 41 P. Dobromirova, A. Endah and M. Ulbricht, *Sep. Purif. Technol.*, 2011, **81**, 124–133.
- 42 Q. She, C. Tang, Y.N. Wang and Z. Zhang, *Desalination*, 2009, **249**, 1079–1087.

### List of Tables

**Table 1:** Composition of different membrane casting solution.

**Table 2:** Some characteristic parameters of fabricated membranes.

### List of Figures

**Figure 1:** Steps for fabrication of PVCL-co-PSF modified membranes.

**Figure 2:** ATR-FTIR spectra of plain and PVCL-co-PSF copolymer blended membranes.

**Figure 3:** Temperature dependent hydration capacity of prepared membranes.

**Figure 4:** Effect of initial quantity of VCL monomer on BSA adsorption and hydrophilicity of prepared membranes.

**Figure 5:** Top surface FESEM images of plain and modified membranes.

**Figure 6:** Cross section SEM images of plain and modified membranes.

**Figure 7:** Effect of initial quantity of VCL monomer on flux profile during compaction (at 300 kPa).

**Figure 8:** Effect of initial quantity of VCL monomer on pressure dependent flux through different membranes.

**Figure 9:** Effect of initial quantity of VCL monomer on (a) BSA flux and rejection values (b) HA flux and rejection values through different membranes.

**Figure 10:** Different flux values through prepared membranes during fouling study with (a) BSA and (b) HA.

**Figure 11:** Schematic representation of mechanism modified hydraulic cleaning.

**Figure 12:** Effect of initial quantity of VCL monomer on different fouling values for prepared membranes during (a) BSA ultrafiltration and (b) HA ultrafiltration.

**Figure 13:** Flux recovery ratio after normal and modified hydraulic cleaning after (a) BSA ultrafiltration and (b) HA ultrafiltration.

### List of Tables

**Table 1:** Composition of different membrane casting solution.

**Table 2:** Some characteristic parameters of fabricated membranes.

### List of Figures

**Figure 1:** Steps for fabrication of PVCL-co-PSF modified membranes.

**Figure 2:** ATR-FTIR spectra of plain and PVCL-co-PSF copolymer blended membranes.

**Figure 3:** Temperature dependent hydration capacity of prepared membranes.

**Figure 4:** Effect of initial quantity of VCL monomer on BSA adsorption and hydrophilicity of prepared membranes.

**Figure 5:** Top surface FESEM images of plain and modified membranes.

**Figure 6:** Cross section SEM images of plain and modified membranes.

**Figure 7:** Effect of initial quantity of VCL monomer on flux profile during compaction (at 300 kPa).

**Figure 8:** Effect of initial quantity of VCL monomer on pressure dependent flux through different membranes.

**Figure 9:** Effect of initial quantity of VCL monomer on (a) BSA flux and rejection values (b) HA flux and rejection values through different membranes.

**Figure 10:** Different flux values through prepared membranes during fouling study with (a) BSA and (b) HA.

**Figure 11:** Schematic representation of mechanism modified hydraulic cleaning.

**Figure 12:** Effect of initial quantity of VCL monomer on different fouling values for prepared membranes during (a) BSA ultrafiltration and (b) HA ultrafiltration.

**Figure 13:** Flux recovery ratio after normal and modified hydraulic cleaning after (a) BSA ultrafiltration and (b) HA ultrafiltration.

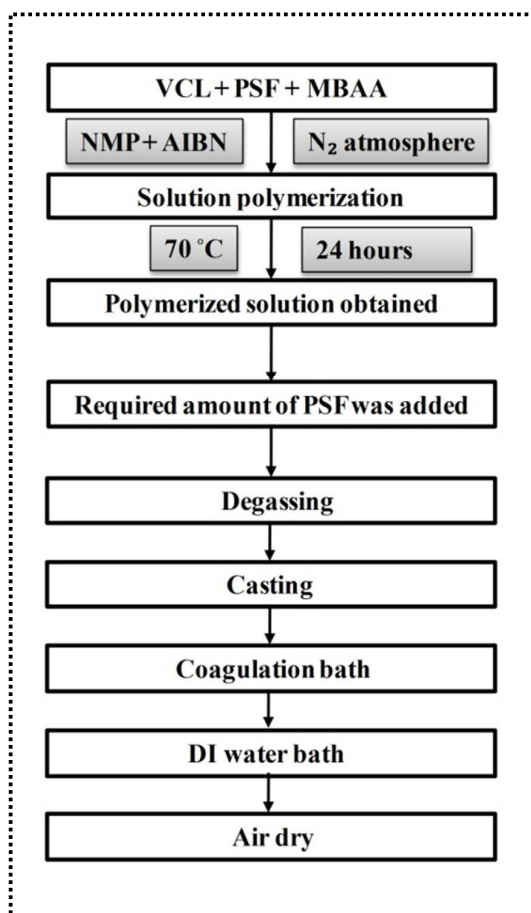


Figure 1

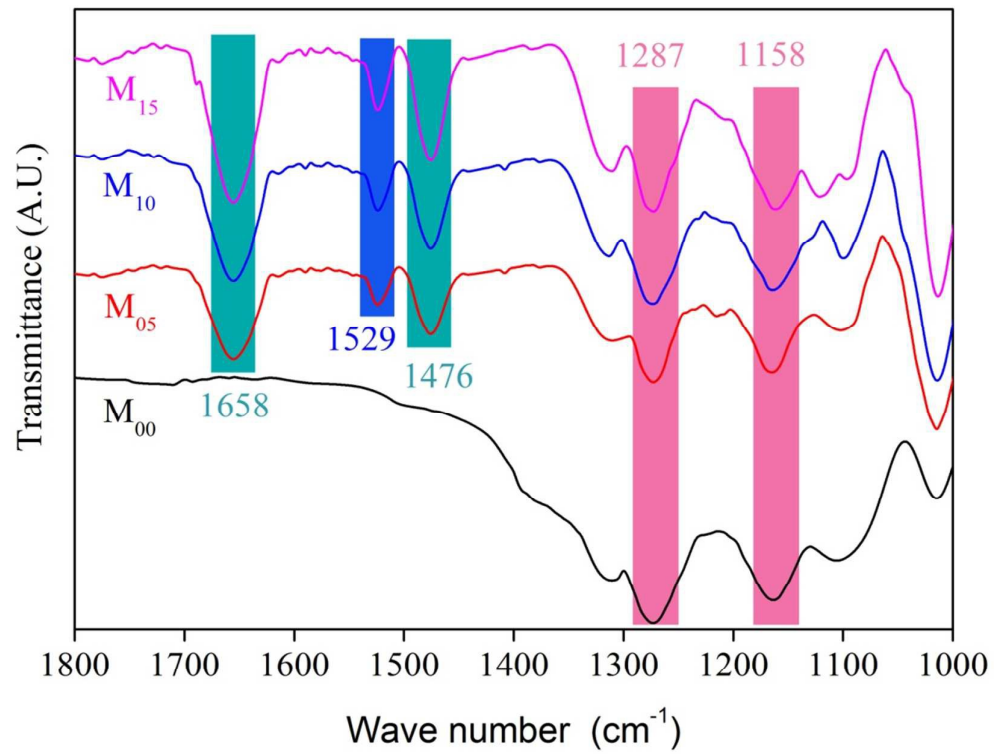


Figure 2

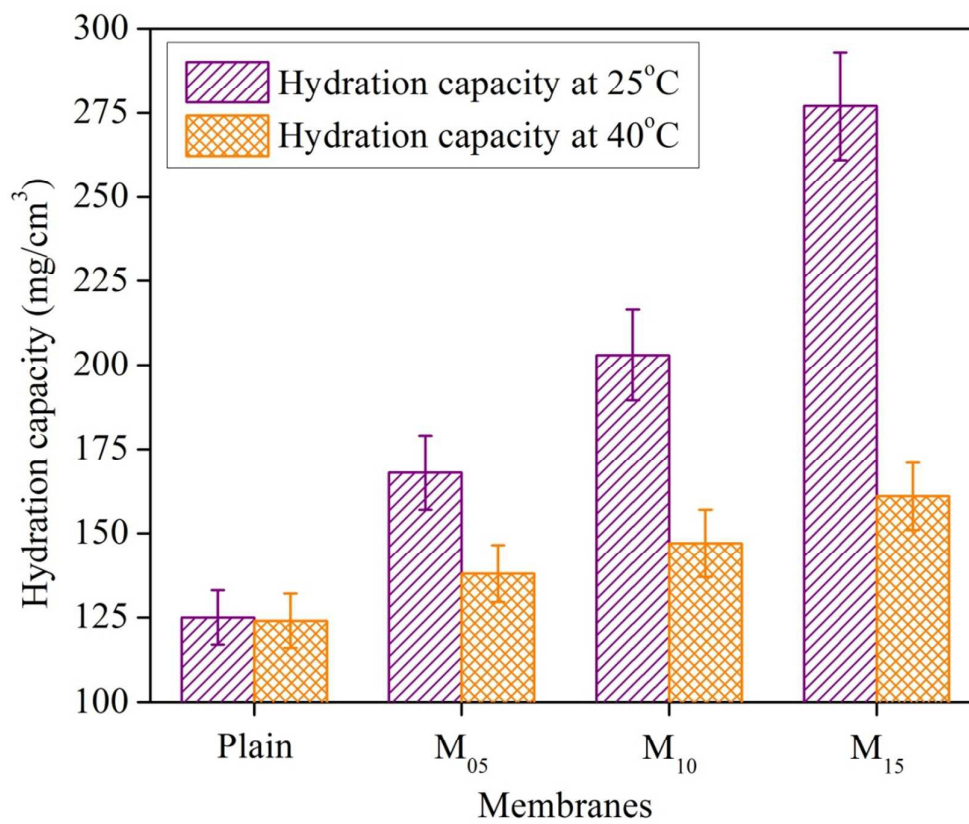


Figure 3

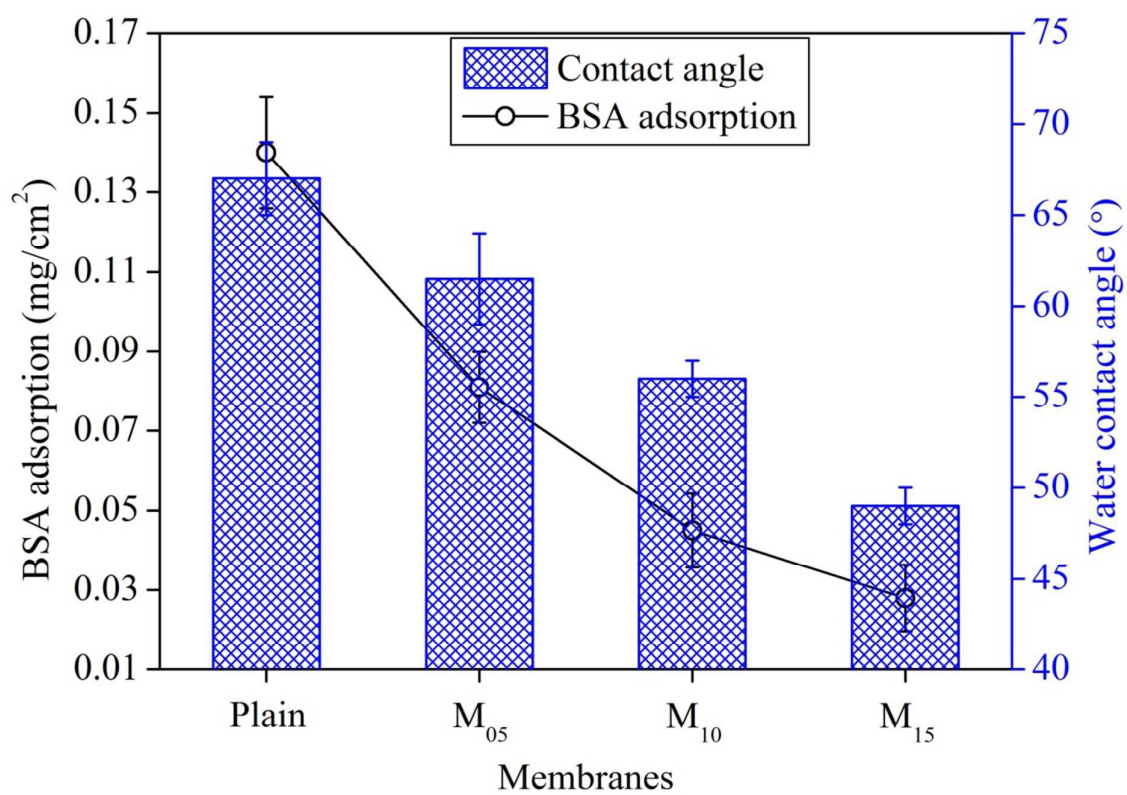


Figure 4

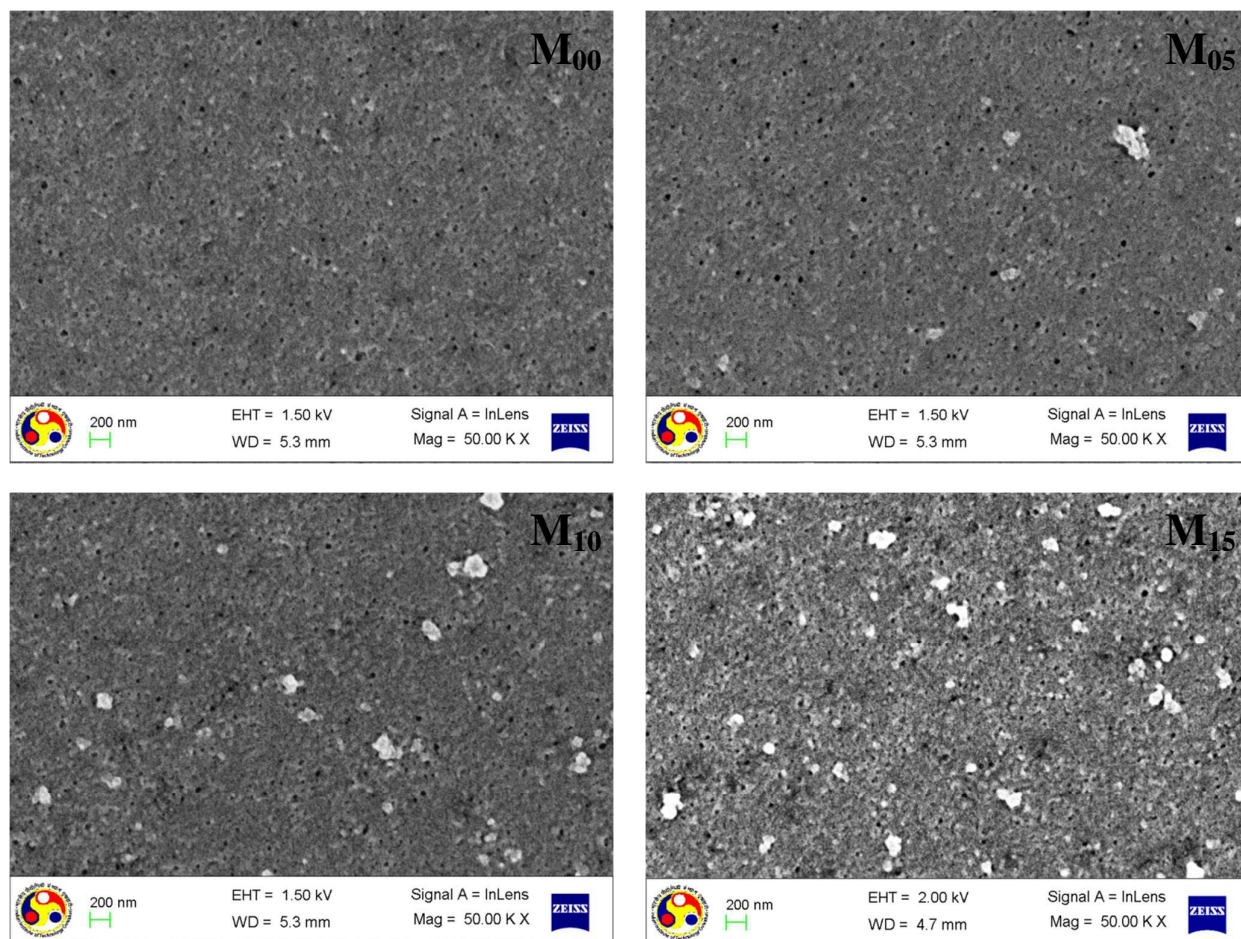
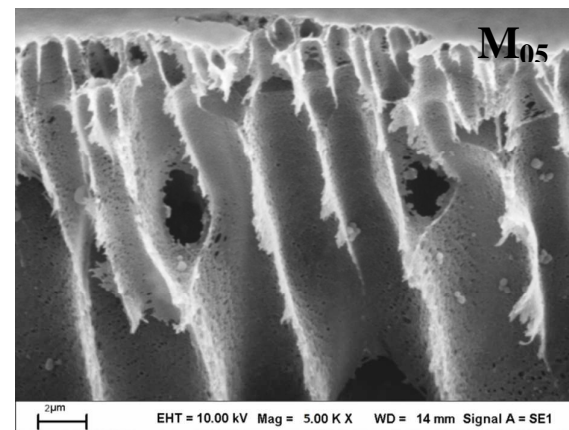
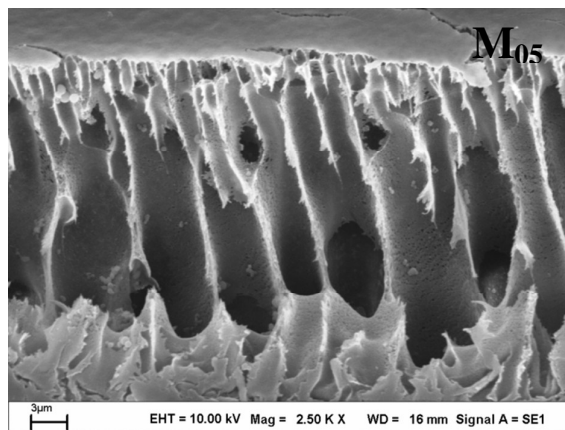
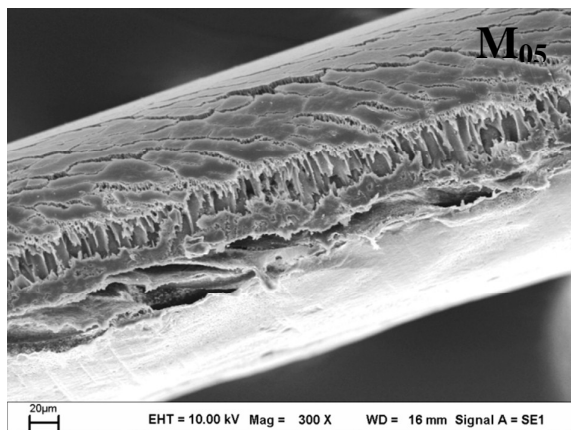
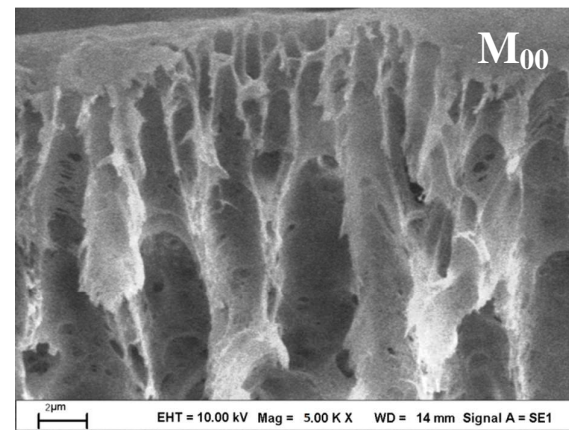
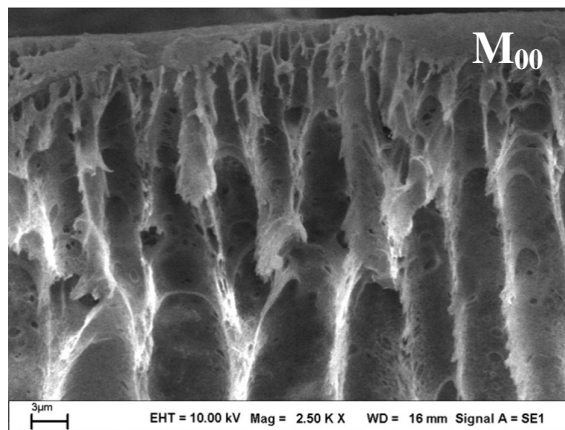
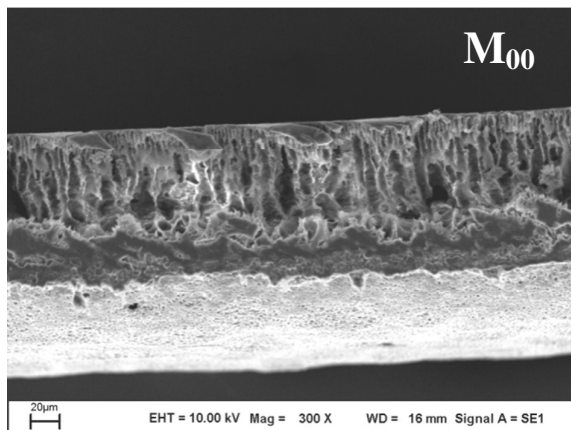


Figure 5





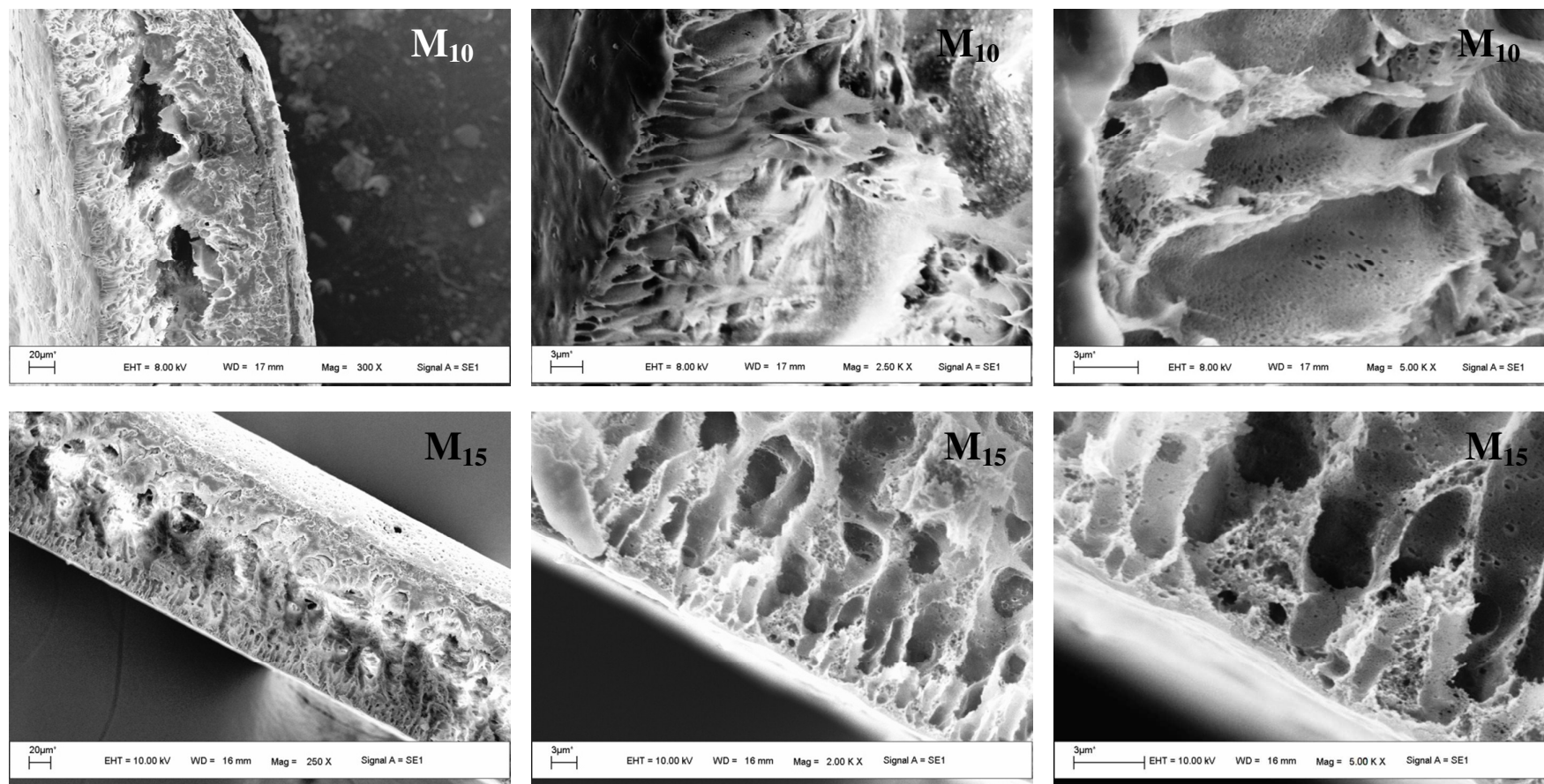


Figure 6

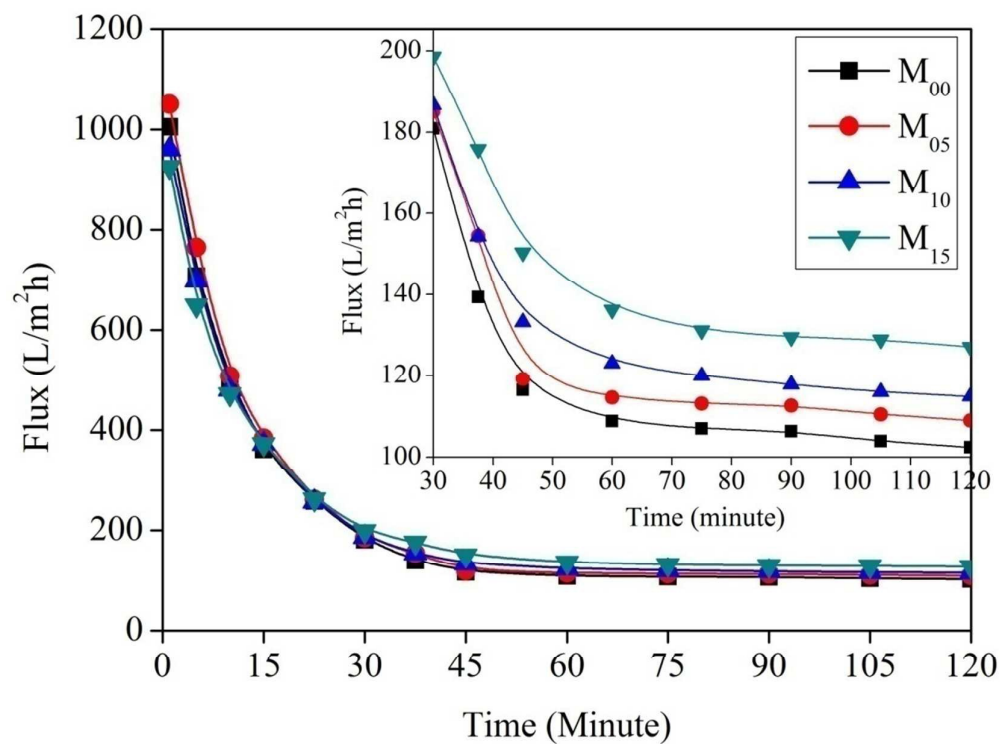


Figure 7

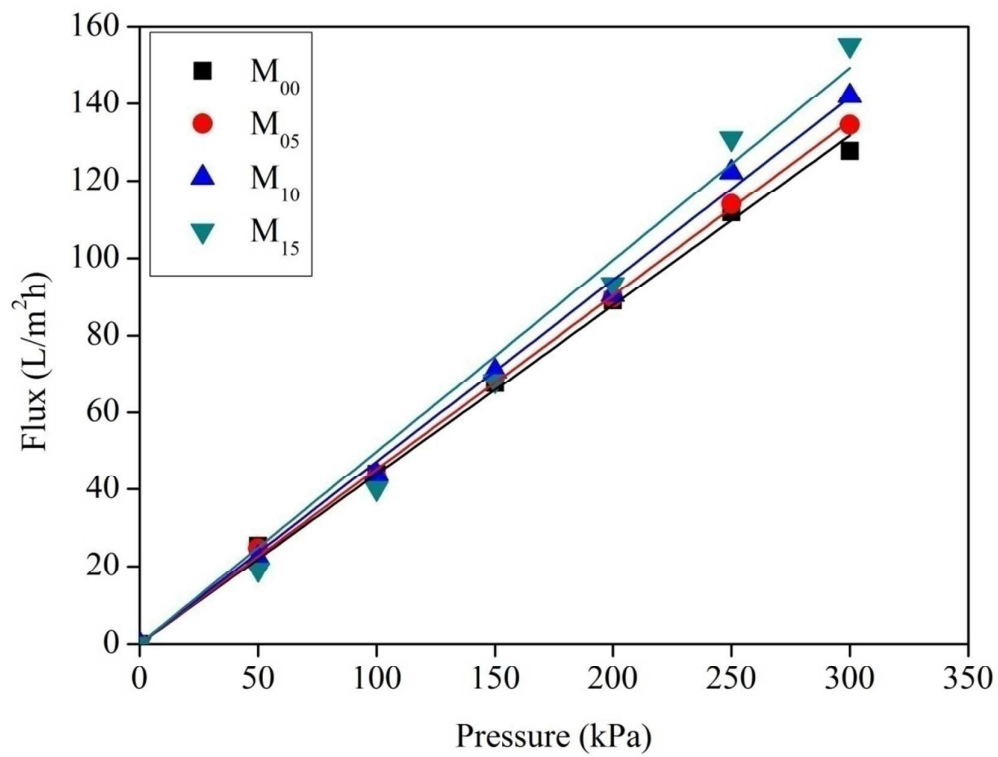
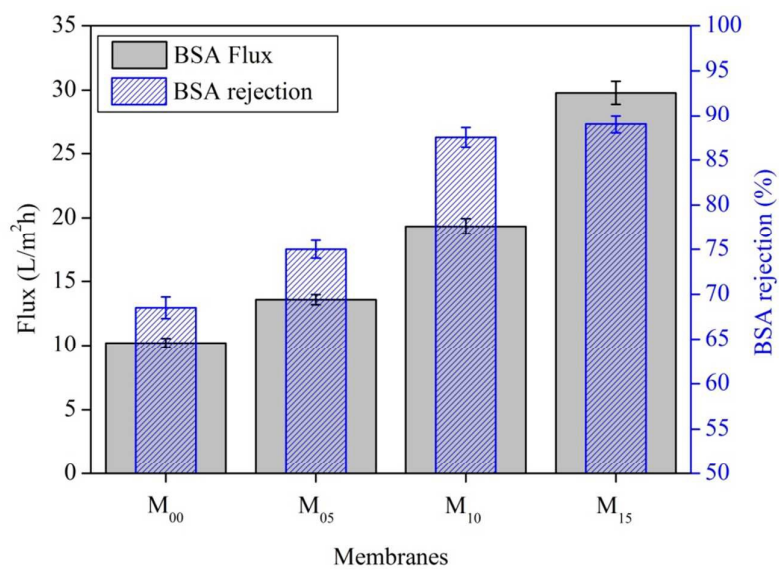
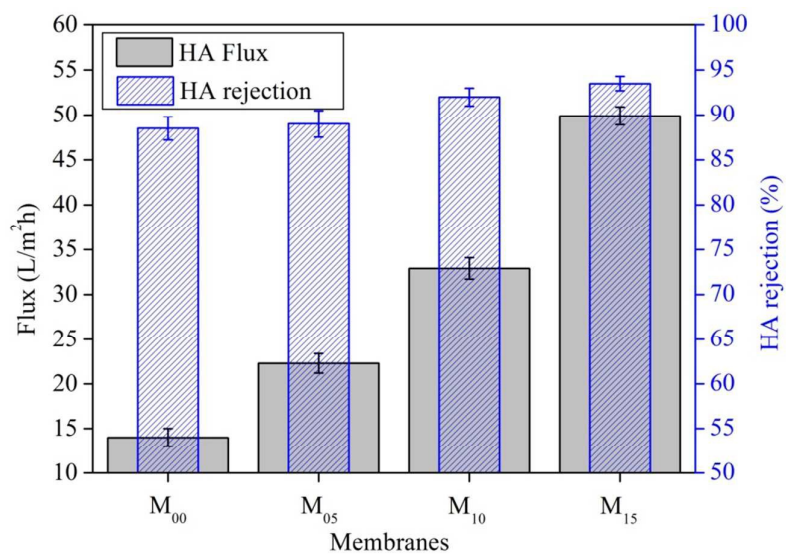


Figure 8

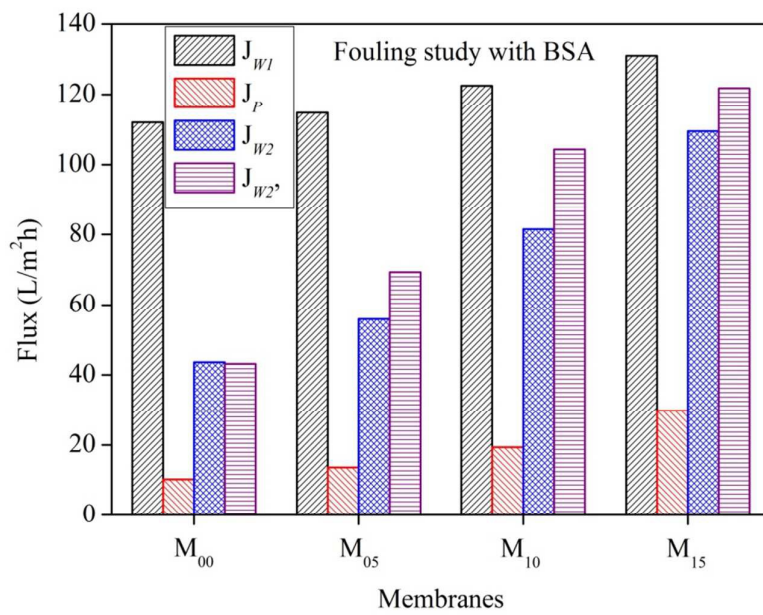


(a)

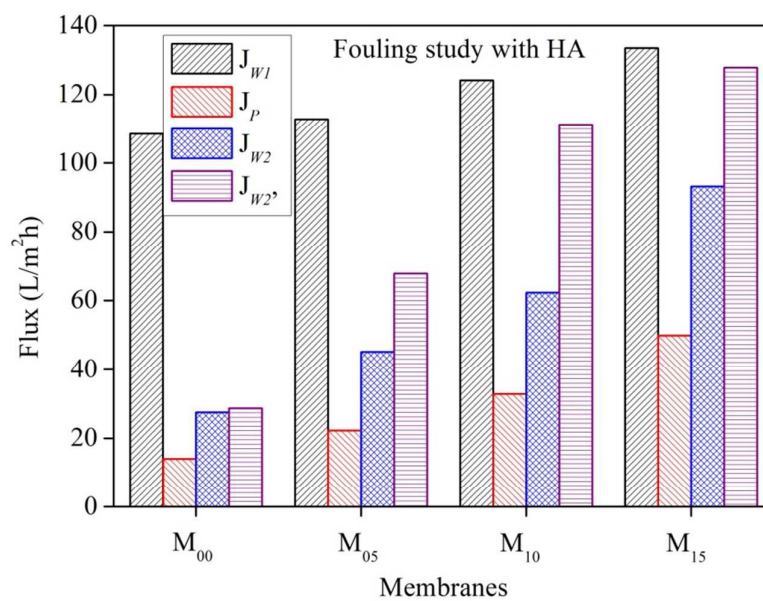


(b)

Figure 9



(a)



(b)

Figure 10

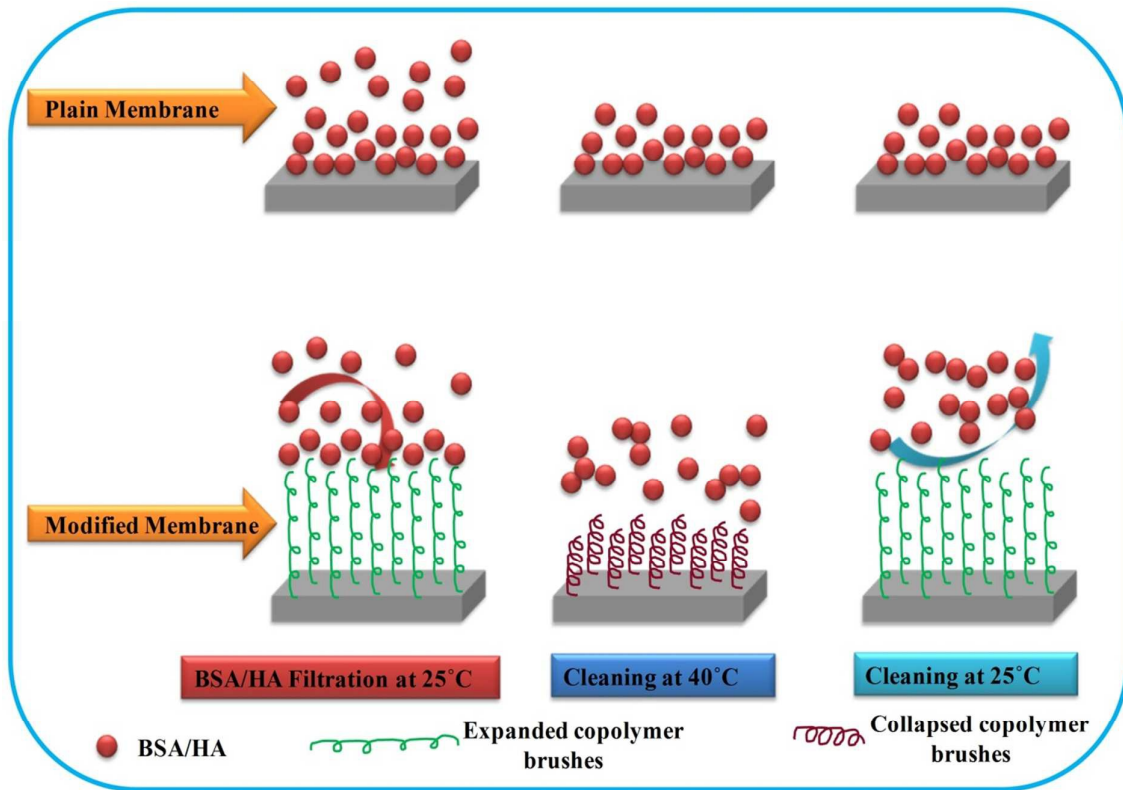
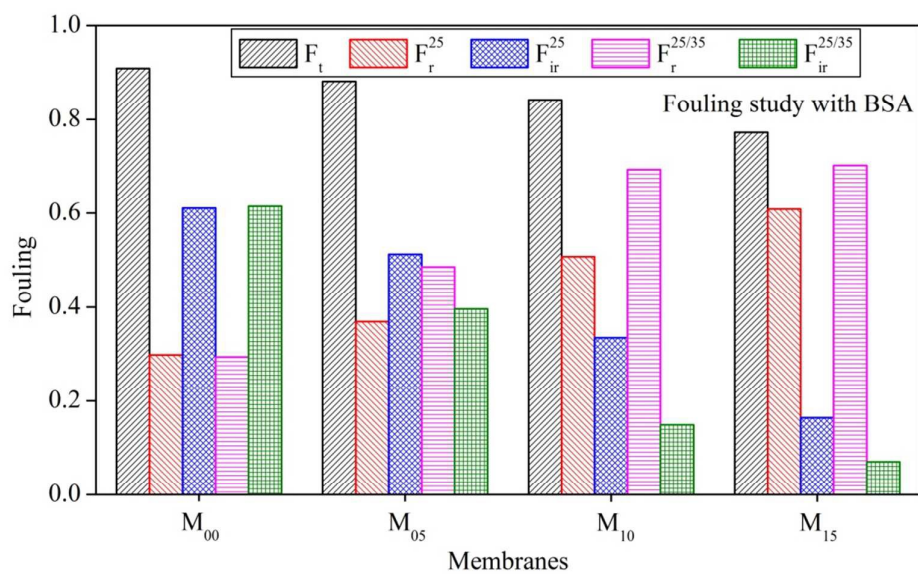
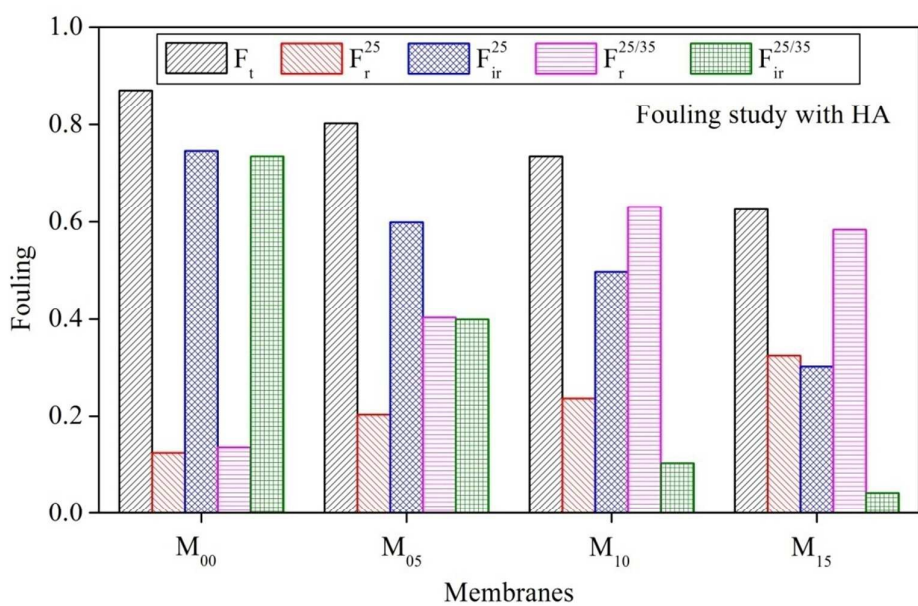


Figure 11



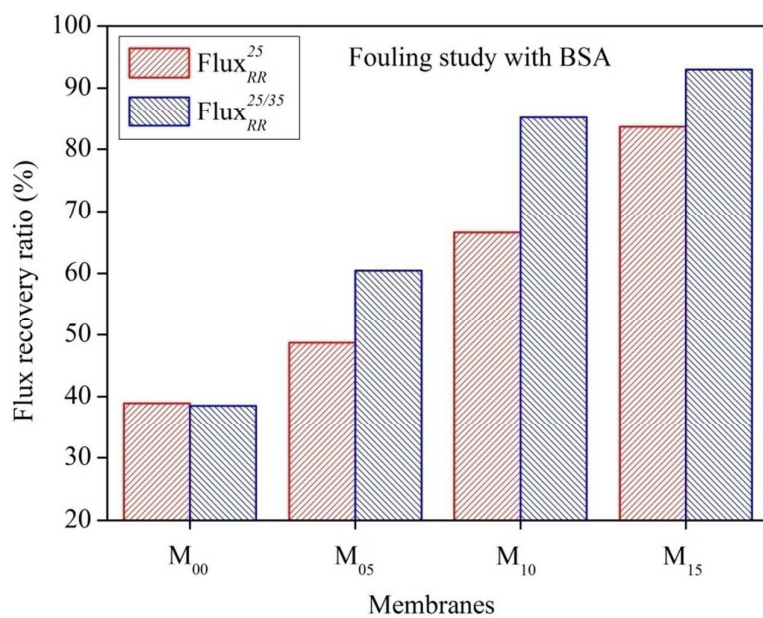
(a)



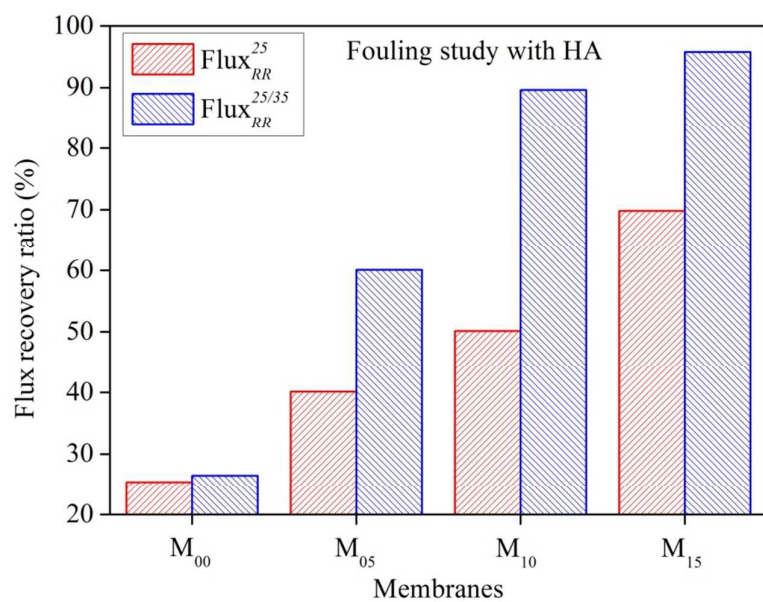
(b)

Figure 12





(a)



(b)

Figure 13

**Table 1: Composition of membrane casting solution**

Membrane solution	Ratio of PSF: VCL	PSF I	VCL	MBAA	PEG 4000	PSF II	NMP
Plain	–	–	–	–	7	15	78
M <sub>05</sub>	2:05	1	2.5	0.35	7	14	75.15
M <sub>10</sub>	2:10	1	5.0	0.6	7	14	72.4
M <sub>15</sub>	2:15	1	7.5	0.85	7	14	69.65

**Table 2: Value of some characterization parameters of prepared membranes**

Membrane	Contact angle (°)	CF	P <sub>m</sub>	Thickness
Plain	67±2	9.85	0.44	109±13
M <sub>05</sub>	61.5±2.5	9.64	0.45	122±15
M <sub>10</sub>	56±1	8.36	0.47	143±12
M <sub>15</sub>	49.5±1	7.28	0.50	157±10